Proceedings of the 50th International School & Conference on the Physics of Semiconductors

Efficient Emission in the Telecom Range from Quantum Dots Embedded in Photonic Structures Fabricated by Focused Ion Beam Milling

M. Jaworski[a,b,*], A. Chudzyńska[b,c], P. Mrowiński[a] and G. Sęk[a]

[a] *Department of Experimental Physics, Faculty of Fundamental Problems of Technology, Wrocław University of Science and Technology, Wybrzeże Wyspiańskiego 27, 50-370 Wrocław, Poland*

[b] *Nanores, Bierutowska 57–59, 51-317 Wrocław, Poland*

[c] *Department of Optical Spectroscopy, W. Trzebiatowski Institute of Low Temperature and Structural Research of the Polish Academy of Sciences, Okólna 2, Wroclaw 50-422, Poland*

Doi: 10.12693/APhysPolA.142.662 *e-mail: maciej.jaworski@pwr.edu.pl

In the present work, we focus on the development and optimization of the photonic structures fabrication with (In,Ga)As/GaAs quantum dots as an active part. Such structures offer the emission in the application-relevant range of the 2nd telecommunication window in view of obtaining efficient light collection, which is a critical requirement of practical, truly nonclassical sources for quantum communication schemes in fiber networks. We fabricated pillar-like photonic structures as a function of the sample and technological process parameters, which were then characterized by low-temperature micro-photoluminescence in order to optimize the emission intensity. We tested two different ion sources (Ga and Xe) also using an additional protection layer of carbon sputtered by the gas injection system. For each source, we have prepared a set of pillars with varying diameters and heights of the order of single micrometers, with fine-tuning of the beam currents and energy, and hence of the ion doses. We concluded that the optimized method should employ the xenon plasma focused ion beam technique, which takes advantage of high milling rate and high quality of etching of small structures, even micrometer in size, on the semiconductor material. For an optimized process, we obtained bright photoluminescence from single quantum dots. Our results indicate the potential of this technological approach employing xenon plasma focused ion beam technique to be suitable for the creation of photonic structures of good crystalline and optical quality, exhibiting efficient emission from embedded quantum dots in the telecommunication spectral range.

topics: plasma focused ion beam, quantum dots, photonic structures, micro pillars

1. Introduction

Considerable interest has recently been given to the development of basic building blocks for nanophotonic and optoelectronic devices that utilize single semiconductor quantum dots (QDs) [1–4]. A combination of bottom–up and top–down nanofabrication processing is a promising approach for the fabrication of a high-quality photonic environment [5]. Focused ion beam (FIB) milling provides a simple one-step approach without the need to optimize the etching conditions, as is the case with commonly used electron beam lithography or photolithography. Moreover, resist-based lithography methods require further processing to complete device manufacture, and so they do not offer the flexibility of quick prototyping, which could be avoided by using maskless FIB processing to structure bulk materials. In this context, photonic micropillar structures with quantum emitting nanostructures [6–9] or subwavelength optics for surface plasmons [10] have already been fabricated. There exists several reports on micropillars cavities realized using FIB processing based on CdTe [8] or GaAs [11] materials systems, which, however, contain a few microns thick multilayer capping of QDs (mostly forming the top distributed Bragg reflector — DBR). The latter protects the inner parts from ion-beam-induced crystalline defects in the vicinity of the optically active material. Our approach focuses on samples with much thinner, single-layer capping, i.e., without DBR on top, as it has been demonstrated that structures that are less demanding and less costly in growth can also offer very good extraction efficiencies over a broad spectral range [12–14]. This is in contrast to sophisticated microcavity structures and has the advantage of significantly lower sensitivity to wavelength matching between the quantum emitter and the maximum of emission extraction driven by the photonic confinement. However, this requires more careful treatment of the sample surface to maintain its high optical quality and special optimization of the ion beam processing. Therefore, we apply the xenon plasma focused ion beam (Xe-PFIB) technology to realize micropillar-like photonic structures, aiming at high and broad extraction efficiency function, which is a rather unconventional approach. The xenon plasma ion beam provides faster milling than Ga-based FIB, and moreover, xenon is nonreactive element, which is very important in the processing of group III–V semiconductors.

We investigate the (In,Ga)As/GaAs structure emitting at 1.3 μm with QDs embedded in the GaAs matrix [14]. The sample was processed with FIB to make various diameters mesa structures, mainly to isolate single QD emission lines, but also to improve the light collection efficiency. We study the optical properties of such photonic structures with the use of a micro-photoluminescence experiment to detect excitonic states of a single QD, focusing on the brightness of the emission as the primary figure of merit of the technological process efficiency. Our work is mainly focused on optimizing FIB milling in terms of reduced sidewall damages, avoiding cone-like etching, and to check how milling parameters influence internal quantum efficiency.

2. Sample structure and fabrication processing

The sample chosen for these studies is based on GaAs substrate and contains, as an active part, self-assembled (In,Ga)As/GaAs quantum dots, grown by metalorganic chemical vapor deposition in the Stranski–Krastanov growth mode. Dots with an areal density of $\sim 10^9$ cm^{-2} are formed on the wetting layer and are covered by a low indium content strain-reducing layer in order to shift the emission wavelength to the 1.3 μm range. For enhanced extraction efficiency of the emitted radiation, QDs are grown on DBR composed of 23 pairs of GaAs/(Al,Ga)As layers on top of the undoped GaAs buffer (300 nm). The thickness of the GaAs layer surrounding the QD layer is designed to form a 2λ cavity between the DBR and the sample surface, while the top GaAs layer is 634 nm thick, which is crucial for FIB processing to minimize ion bombardment inducing damage in the crystal in the vicinity of the active layer. A sample layout is shown in Fig. 1, while more details about the structure properties of QDs have been described elsewhere [14–17].

The fabrication processing step is realized with the use of Xe-PFIB with an inductively coupled plasma ion parallel source. The apparatus used was the Helios G4 PFIB CXe Dual Beam combined with the second scanning electron microscope (SEM) column. The implantation of atoms in the crystal structure of the III–V semiconductor alloy using xenon plasma is expected to be less efficient than in the case of a similar FIB system using gallium ions.

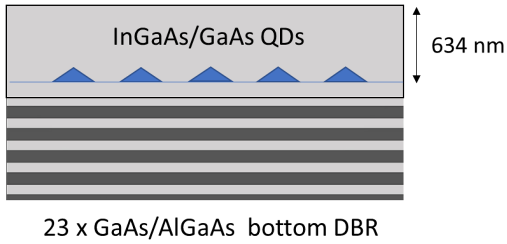

Fig. 1. (a) Schematic sample layout containing (In,Ga)As QDs on top of the DBR structure which consist of 23 layers of GaAs and (Al,Ga)As.

The main reason is related to the smaller penetration depth of Xe ions, as demonstrated in Fig. 2 by simulations using the Stopping and Range of Ions in Matter (SRIM) software [18] in both cases (see Fig. 2). The results shows that the use of Xe ions is expected to be much less damaging to the processed GaAs material. With the Xe ion beam current in a range from 1.5 pA to 2.5 μA, the process is robust and fast in the context of the fabrication processing of the pillar microstructures with few microns in diameter. The sample is mounted on a standard SEM holder and stuck with copper tape, which also enhances discharge of the surface.

The first pillars (see the exemplary SEM image in Fig. 3a) were created using Ga-FIB for reference only, in order to realize micropillars in a methodology analogous to that reported in the literature [11]. For rough milling, the ion beam current of 1 nA and the beam energy of 30 keV were used, which is the first process of removing a huge amount of material in a very fast pace, therefore a high beam current of the order of nA is needed. Next, as shown in Fig. 3b, pillars were made with the same beam parameters as the one in Fig. 3a, but with an additional polishing step using the beam current of 11 pA to make the shape more cylindrical, and to obtain more vertical and smoother sidewalls. The micropillar shown in Fig. 3c was created with the use of Xe-PFIB with an energy of 30 keV, ion beam current 4 nA and dose of 9.8×10^{-9} pC/μm^2, which results in a characteristic conical shape due to the broader spot size of the xenon ion beam. It is worth noting that both the top of the pillar and the edges of the milled area indicate amorphization, which is due to the fact that some of the atoms evaporated from the target sample sticks to the surface, which is a redeposition process. For all pillars, as the examples in Fig. 3a–c, we observed a complete degradation of the photoluminescence signal, which led us to the step with applying a protective layer. The last micropillar shown in Fig. 3d was made with the use of Xe-PFIB and with a protective carbon layer (100 nm thick), made by gas injection system using a carbon precursor. The carbon layer was actually used to protect the quantum dots from ion implantation and to preserve the photoluminescence intensity. As it has been observed in the SEM images,

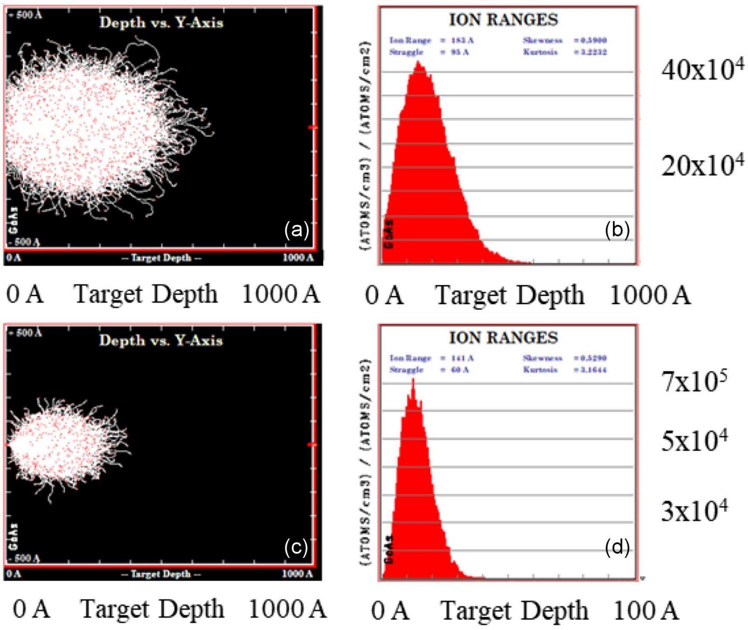

Fig. 2. SRIM calculations for amorphic GaAs as a target with a 30 keV ion beam for both depth penetration around 100 nm and ion range distribution for gallium ion source (a), (b) and for xenon ion source (c), (d).

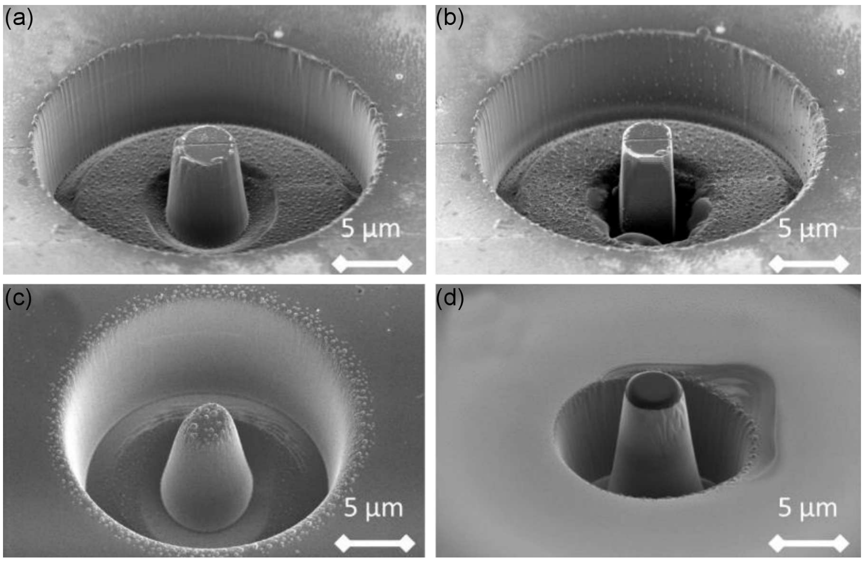

Fig. 3. (a)–(d) Micropillar samples realized by applying focused ion beam milling. The samples in (a) and (b) are made with Ga-FIB and differ in ion beam current, while the samples (c) and (d) are obtained with Xe-PFIB. The sample (d) contains a carbon layer on top for protection (see text for more details of processing).

the additional carbon layer also influences the micropillar sidewalls making them smoother. The disadvantage of using a protective carbon layer, however, is the noticeable loss of QD luminescence when compared to the areas of the unprocessed sample, while the removal of the carbon layer, which can be realized by plasma cleaning, turned out to be a fully destructive process.

The main difference between the two ion sources in double beam systems (i.e., between Ga-FIB and Xe-PFIB), is the characteristic spot size of the ion beam as a function of the ion beam current. The dependence of the spot size of the ion beam for the liquid metal of the gallium ion source and the inductively coupled plasma of xenon ions was investigated and for the 1 nA xenon beam it is two times larger as the gallium beam [19] — the spot size of Xe-PFIB is more stable for higher currents (from 50 nA to even 1 μA). In contrast, in the case of Ga-FIB, spot size increases very quickly for currents above 50 nA. That is why if the material of the structure can withstand the energy of the ion beam of 30 keV and currents above 50 nA, Xe-PFIB would be the most efficient way to fabricate the structures with a very short processing times (few minutes) overall. Moreover, in the case of low currents, the plasma-focused ion beam of xenon still has a small enough spot size to perform fine polishing, although it is not as small as the spot size of the gallium ions, which for the picoampers current reaches the size even below 10 nm.

3. Optical characterization

Microphotoluminescence measurements were performed at low temperature (5 K) — the sample was mounted on a cold finger in a liquid-helium continuous-flow cryostat. It was excited nonresonantly with the 660 nm line of a continuous wave (cw) semiconductor laser diode. Both the excitation and the emission is transmitted via a microscope objective with a long working distance with a numerical aperture of 0.4. The QD emission is further spectrally resolved with a 1 m focal-length monochromator with a 150 or 600 grooves/mm gratings (different spectral resolutions) and detected using a liquid-nitrogen-cooled (In,Ga)As multichannel linear detector. The setup provides effectively a spectral resolution of at least 25 μeV for the 600 grooves/mm grating, and a spatial resolution of a spot with a diameter of several μm. This allows to excite precisely one pillar at a time and to spectrally resolve single quantum dot emission lines.

According to our preliminary studies on the samples shown in Fig. 3 and taking into account the features of all described methods, we can conclude that the approach of using a double beam microscope SEM/Xe-PFIB is more promising for the design of an efficient quantum light source based on single quantum dots. Therefore, in the next steps, we skipped the use of the top carbon layer and instead focused on optimizing the FIB process as itself compared to those corresponding to Fig. 3c. In the following steps, we selected new places on the sample and in the eccentric position, we set the ring-shaped patterns with the inner(outer) diameter in the following sequence: s1 with 10(20) μm; s2 with 15(30) μm; s3 with 5(15) μm. The dwell time of the ion beam was set to 1 μs and the beam passing mode was set from the outer position to the inner position which results in a polished surface of a pillar even in the case of a rough milling process. As described above, our sample layout consists of a 634 nm thick top GaAs capping layer, so our target pillar height was set to 1 μm to ensure the active QD layer etching, and to limit the number of quantum dots that will be optically excited inside a single pillar. The milling process has been optimized by decreasing the ion beam current to limit structure degradation by lowering the amount of ions absorbed by the target in entire time of the process, that is why milling is realized with the beam energy set to 30 keV and the ion beam current of 1 nA. Using these settings,

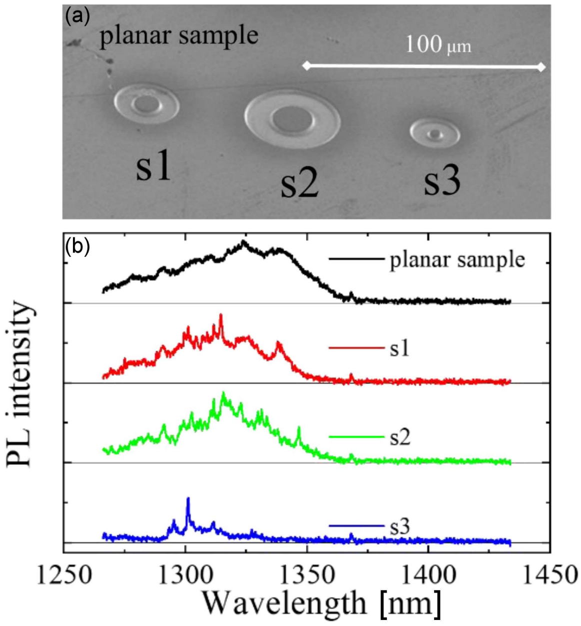

Fig. 4. SEM image of structures made by Xe-PFIB with various inner diameters of 10, 15, and 5 μm for s1, s2, and s3, respectively. The height of the pillars is 1 μm. (b) The μ-photoluminescence spectra taken for all three samples and for a planar region of a sample as a reference.

the dose applied to the surface was estimated by the microscope software to 2.3×10^{-9} pC/μm^2. The time required to create such micropillar structures was approximately 9 min for s1, 20 min for s2, and 6 min for s3. The SEM images of the realized micropillar samples are shown in Fig. 4a. In Fig. 4b, we demonstrate the photoluminescence (PL) spectra taken for all three samples and for the reference position in the planar (unprocessed) region of the sample. The spectra of all micropillars show emission lines of single QDs (in contrast to PL from the planar part) as the number of optically active QDs is limited by FIB processing. However, for s1 and s2 sample, the number of QDs is still too high to fully isolate single QD emission lines. After decreasing the size of the micropillar to 5 μm in diameter, as in the s3 sample, the spectra show only a few optical transitions, even with the use of a rather moderate optical excitation power of 20 μW and a low resolution grating. It is worth noting that the optical transition seen around the wavelength of 1300 nm for the sample s3 characterizes a similar intensity level as observed for the planar sample, in which the QD ensemble is excited. Compared to the number of counts we observed on similar samples in our previous work [20] and after optimizing the micropillar dimensions, the number of counts observed for sample s3 on single photon counting modules, based on a superconducting nanowire detection system, would be sufficient for further studies in terms of purity and indistinguishability of single photons.

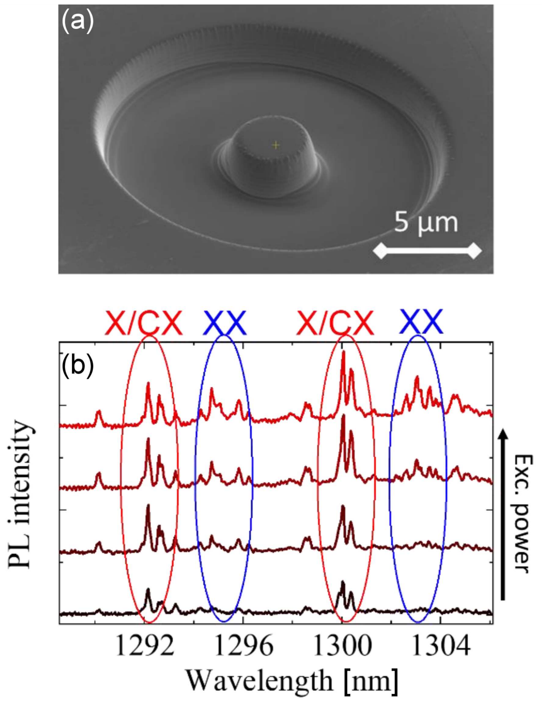

Fig. 5. (a) SEM micrograph of a micropillar sample investigated in a more detailed manner using high spectral resolution micro-photoluminescence experiment. (b) Recorded spectra of quantum dots emission for various excitation powers.

Next, we performed the μPL experiment with high spectral resolution on the pillar s3. Figure 5a shows a magnified SEM image of this micropillar with characteristic round edges resulting from a wide beam of xenon plasma ions. The PL spectra are shown in Fig. 5b. Here we used a series of excitation powers ranging from 0.1 μW to 10 μW to determine typical features of the single QD emission. For a lower excitation power, we observe just a few optical transitions, most probably related to different QDs. At this stage, we did not pursue the characterization to distinguish unequivocally between certain excitonic complex states. Indeed, we observe more spectral lines appearing, the excitation power intensity of which increases faster, while those observed at low excitation tend to saturate. A faster increase of the intensity is an indication of biexciton state (XX), and a saturation of intensity suggests neutral exciton (X) or charged exciton (CX) state, as it is assigned in Fig. 5b. In fact, further polarization-resolved studies are needed, or measurements of cross-correlations in the second order photon emission correlation function, which were out of the scope of this work, focusing rather on the processing method development. It has been proven that, first of all, the intensity of the emission from selected optical transitions from micropillar fabricated by the specially optimized Xe-PFIB is high enough to probe the single photon emission at the second telecommunication window from such structures.

4. Conclusions

We fabricated a set of micropillar structures with (In,Ga)As/GaAs quantum dots by applying FIB. Various approaches were tested and analyzed in context of roughness of top plane and sidewalls, and then intensity of the QD emission. This allowed us to select the XFIB method as offering the best compromise between good quality of the sample maintaining a defect-free layer of QDs embedded inside, and the efficiency of the entire fabrication procedure. For the micropillar structures obtained in the optimized process, the micro-photoluminescence experiment does not show a significant degradation of the luminescence intensity related to ion implantation-induced amorphization when compared to the unprocessed areas. Moreover, for the case of a micropillar with a diameter of 5 μm, we are able to resolve optical transitions associated with radiative recombination of excitonic states in single quantum dots in the spectral range of 1.3 μm. The obtained bright emission implies a sufficient light extraction efficiency towards the top direction (and the collection optics), which is due to both the bottom distributed Bragg mirror and the in-plane optical confinement of the pillar. Therefore, we expect that such processing is a promising method for the realization of efficient single photon source emitting in the telecommunication windows.

Acknowledgments

This work has been supported by the "Implementation doctorate" program of the Polish Ministry of Education and Science within grant No. DWD/4/50/2020. We would like to thank Stephan Reitzenstein from Technische Universität Berlin for providing the semiconductor quantum dot materials used for this study within the Academic Partnership Programme funded by the Polish National Agency for Academic Exchange within project No. PPI/APM/2018/1/00031/U/001.

References

[1] H. Wang Y.-M. He, T.-H. Chung et al., *Nat. Photon.* **13**, 770 (2019).

[2] T. Müller, J. Skiba-szymanska, A.B. Krysa, J. Huwer, M. Felle, M. Anderson, R.M. Stevenson, J. Heffernan, D.A. Ritchie, A.J. Shields, *Nat. Commun.* **9**, 862 (2018).

[3] L. Hanschke, K.A. Fischer, S. Appel, D. Lukin, J. Wierzbowski, S. Sun, R. Trivedi, J. Vučković, J.J. Finley, K. Müller, *Npj Quantum Inf.* **4**, 43 (2018).

[4] J. Liu, K. Konthasinghe, M. Davanço et al., *Phys. Rev. Appl.* **9**, 064019 (2018).

[5] J.-S. Huang, V. Callegari, P. Geisler et al., *Nat. Commun.* **1**, 150 (2010).

[6] H. Lohmeyer, J. Kalden, K. Sebald, C. Kruse, D. Hommel, J. Gutowski, *Appl. Phys. Lett.* **92**, 011116 (2008).

[7] M. Karl, S. Li, T. Passow, W. Löffler, H. Kalt, M. Hetterich, *Opt. Express* **15**, 8191 (2007).

[8] W. Pacuski, T. Jakubczyk, C. Kruse et al., *Cryst. Growth Des.* **14**, 988 (2014).

[9] W.-M. Schulz, T. Thomay, M. Eichfelder, M. Bommer, M. Wiesner, R. Roßbach, M. Jetter, R. Bratschitsch, A. Leitenstorfer, P. Michler, *Opt. Express* **18**, 12543 (2010).

[10] W.L. Barnes, A. Dereux, T.W. Ebbesen, *Nature* **424**, 824 (2003).

[11] Y.-L.D. Ho, R. Gibson, C.Y. Hu, M.J. Cryan, J.G. Rarity, *J. Vac. Sci. Technol. B* **25**, 1197 (2007).

[12] A. Musiał, M. Mikulicz, P. Mrowiński, A. Zielińska, P. Sitarek, P. Wyborski, M. Kuniej, J.P. Reithmaier, G. Sęk, M. Benyoucef, *Appl. Phys. Lett.* **118**, 221101 (2021).

[13] P. Mrowiński G. Sęk, *Phys. B Condens. Matter* **562**, 141 (2019).

[14] N. Srocka, A. Musiał, P.-I. Schneider et al., *AIP Adv.* **8**, 085205 (2018).

[15] P. Mrowiński, A. Musiał, K. Gawarecki et al., *Phys. Rev. B* **100**, 115310 (2019).

[16] P. Podemski, A. Musiał, K. Gawarecki et al., *Appl. Phys. Lett.* **116**, 023102 (2020).

[17] P. Holewa, M. Burakowski, A. Musiał, N. Srocka, D. Quandt, A. Strittmatter, S. Rodt, S. Reitzenstein, G. Sęk, *Sci. Rep.* **10**, 21816 (2020).

[18] J.F. Ziegler, M.D. Ziegler, J.P. Biersack, *Nucl. Instrum. Methods Phys. Res. B* **268**, 1818 (2010).

[19] M.M.V. Taklo, A. Klumpp, P. Ramm, L. Kwakman, G. Franz, *Microsc. Anal.* **25**, 9 (2011).

[20] Ł. Dusanowski, P. Holewa, A. Maryński et al., *Opt. Express* **25**, 31122 (2017).